Dynamic short- and large-coherence interferometry to characterize the induced vibrations and topology change of the cryogenic mirror of the Einstein Telescope prototype

Jesús Vilaboa Pérez, Jérôme Loicq

Jesús Vilaboa Pérez, Jérôme Loicq, "Dynamic short- and large-coherence interferometry to characterize the induced vibrations and topology change of the cryogenic mirror of the Einstein Telescope prototype," Proc. SPIE 12137, Optics and Photonics for Advanced Dimensional Metrology II, 121370T (20 May 2022); doi: 10.1117/12.2622903

SPIE.

Event: SPIE Photonics Europe, 2022, Strasbourg, France

Dynamic short- and large-coherence interferometry to characterize the induced vibrations and topology change of the cryogenic mirror of the Einstein Telescope prototype

Jesús Vilaboa Pérez[a] and Jérôme Loicq[a,b]

[a]Centre Spatial de Liège (CSL), Université de Liège, Avenue du Pré-Aily, 4031, Liège, Belgium
[b]Faculty of Aerospace Engineering, Delft University of Technology, Delft, 2629 HS, Netherlands

ABSTRACT

The E-TEST project builds a prototype for the Einstein Telescope (ET). ET is a proposed gravitational-wave observatory. E-TEST includes a silicon mirror of 30 cm up to 40 cm diameter, suspended and cooled down at cryogenic temperatures from 20 K to 30 K. During the cooling down, the mirror will be affected by surface topology changes, wavefront deformation, and induced vibrations. We present a metrology device based on short-coherence interferometry to characterize the mirror surface with a sub-nanometer resolution. We design an innovative phase mask to achieve dynamic or single-frame white light interferometry. Moreover, we discuss different interferogram analysis methods. We also discuss the implementation of a long-coherence source to facilitate the measurements with the low-coherence source.

Keywords: White Light Interferometry, Dynamical Phase Shifting Interferometry, Single-Frame low-coherence Interferometry, Phase Mask, Measurement of vibrations with interferometry

1. INTRODUCTION

In 2015, the Laser Interferometer Gravitational-wave Observatory (LIGO) detected the gravitational waves for the first time. The next step in the characterization of these waves, generated by the highest energetic processes in the Universe, is the development of the Einstein Telescope. The Einstein Telescope EMR Site Technology (E-TEST) project aims to realize a cryogenic damping prototype for the Einstein Telescope. E-TEST includes a silicon mirror of 30 cm up to 40 cm diameter, suspended and cooled down at cryogenic temperatures around 20 K.[1] During the cooling down, the mirror may be affected by surface topology changes and induced vibrations. H. Kaneda et al. proved the topology change of a large mirror at cryogenic temperatures.[2] In the framework of the Einstein Telescope, the mirror characterization will be essential to ensure the accuracy of the results on the detection of gravitational waves. We describe the state of development of a single-frame white light interferometer to characterize the cryogenic mirrors for a Gravitational Wave detector. The instrument will reach a sub-nanometer resolution in the characterization of the mirror topology. The local and global vibration will be also measured. We propose an interferometer based on a Michelson Interferometer optical layout that uses a white light source of low-temporal coherence. The source will have a bandwidth larger than 100 nm and a centre wavelength at 550 nm. The interference pattern obtained with a low-coherence source is characterized by a well-differentiated central fringe. This zero-order fringe is visible only in a region close to the surface of the measurement point[3,4] As a result, with a white light interferogram, it is possible to unambiguously determine the position of the mirror in contrast with the sinusoidal pattern created by a high-coherence source. In addition to this, low-coherence interferometry avoids spurious unwanted interferometry signals from scattered rays, speckle, dust, imperfections on the optical surfaces that may interfere with the measurement beam. Hence, white light interferometry produces a lower coherent noise and lower phase noise than monochromatic laser-based systems.[5]

To avoid unwanted disturbances, we design an innovative phase mask to perform dynamic or single-frame interferometry. With this phase mask, we can obtain a set of full white light interferograms at each camera

Further author information: (Send correspondence to J.V.P.)
J.V.P.: E-mail: jvilaboaperez@uliege.be

Optics and Photonics for Advanced Dimensional Metrology II, edited by Peter J. de Groot, Richard K. Leach, Pascal Picart, Proceedings of SPIE Vol. 12137, 121370T
 · 0277-786X · doi: 10.1117/12.2622903

frame. The concept of dynamical interferometry has been the object of several studies. Reference[6] summarizes some of these techniques. In addition to this, Pavliček P. et al. recently presented a metrology instrument based on white light interferometry that uses a built-in fibre stretcher to change the optical path difference without mechanical scanning components.[7] The fibre stretcher modulates the spectrum of the white light source and modifies its spectral period for the scanning process. On the other hand, Ferrec Y. et al. presented the concept of a phase mask for interferometry based on a set of Fabry Perot Interferometers of different cavity widths.[8] In our case, it is not feasible to use such a configuration since a Fabry Perot interferometer does not create negative OPDs, which are necessary for white light interferometry to identify the position of the central fringe of the pattern.

With the interferograms captured, the next step is to determine the peak of the coherence envelope that wraps the zero-order fringe. In general, there are two broad methods for this peak detection. The first looks directly for the highest point of the envelope.[9] The second one is a more sensitive method based on the study of the white-light interference phase.[3] In the first group, we can find the well-known centroid method, while in the second group, there is the Phase Shifting Interferometry method and techniques that perform a Fourier analysis of the interference data[4].[3] A phase shift is introduced not only by changing the optical path of the rays but also by a cyclic change in the polarization of the light beam.[10] In our case, we select the method that adapts better to our phase mask design. In Section 2.5, we explain some limitations that we found on these traditional methods when used together with the mask. This limitation drives us to derive new approaches and mathematical functions.

We aim to test some of the innovative features of the metrology instrument by developing a proof of concept at the laboratory. Here we present the instrument concept and the results of the first simulations.

2. METHODS

2.1 Equations that define the white light interference pattern

If we assume that the white light source has a Gaussian power spectrum, the interference pattern can be defined as the combination of the normal probability density function and the fundamental equation of interferometry,[11][12][13] obtaining Eq. 1.

$$I(OPD) = 0.5 \cdot I_0 \cdot \left(1 + \exp\left[-\left(\frac{OPD}{lc}\right)^2\right]\right) \cdot \cos\left(2 \cdot k_0 \cdot OPD\right) \tag{1}$$

Where k_0 is the angular wavenumber: $k_0 = 2\ \pi/\lambda$, with λ the central wavelength of the source; while lc is the coherence length defined in Eq. 2.[14] The coherence length defines the distance the wave travels before the temporal coherence values zero.[5] As a result, the peak of the white light interference pattern is only visible if the OPD between the two arms of the interferometer is less than half the coherence length of the source. The white light pattern has a periodic modulation with a period of $\lambda/2$.

$$lc = \frac{\sqrt{\ln(2)} \cdot \lambda_0^2}{\pi \cdot FWHM(\lambda)} \tag{2}$$

We defined the Full Wave Half Maximum (FWHM) at the 1/e of the highest point of the coherence envelope of the interference pattern, obtained by the exponential function in Eq. 3.

$$\text{Coherent envelope} = \exp\left[-\left(\frac{OPD}{lc}\right)^2\right] \tag{3}$$

With the previous equations, we can define a perfect white light pattern like in Fig. 1.

2.2 Measurement of local vibrations

The initial position of the suspended silicon mirror is unknown due to its non-perfect stability. To compute the local vibration, we use the pair of interferograms measured in two consecutive camera frames. First, we precisely determine the peak of the coherence envelope of each pattern with one of the procedures described in section 2.5. Then, we compute the local vibration between two frames as the distance between the two peaks identified. This distance should be zero on an ideal case where the mirror is perfectly isolated from vibrations. We illustrate the procedure in Fig. 1. On this figure we normalize the intensity to a value between -1 to 1, but the intensity values are always positive. Finally we apply the method to the consecutive pair of camera frames for each of the points inside the area observed.

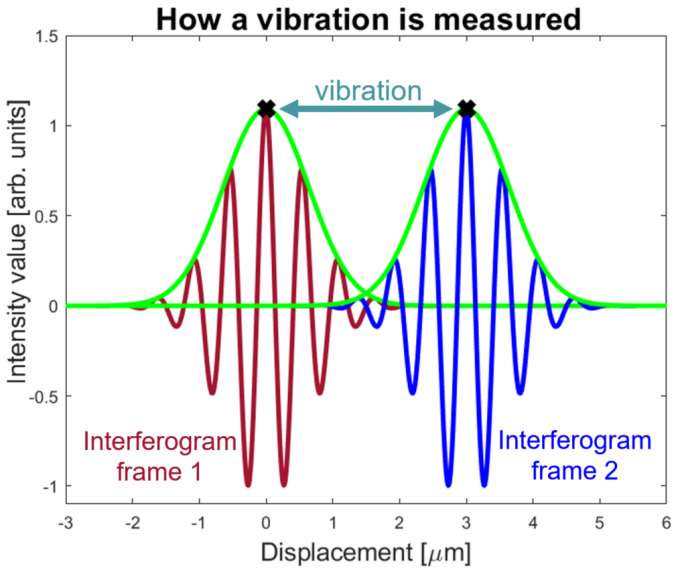

Figure 1. Displacement of the interference pattern between two consecutive camera frames due to vibration.

On the other hand, we compute the change in the mirror topology by processing several of the interferograms obtained at each frame. This procedure allows distinguishing a local topology change from a local vibration. The measurement of local vibrations is one of the most significant advantages of the instrument we propose.

2.3 Optical layout of the instrument

We base our metrology instrument on the optical layout of a Michelson Interferometer. First, we illuminate the mirror with a short-coherence source. Then, the reflected rays will go through several lenses to ensure that the entire FOV passes by all the steps of the phase mask. For this, we use a microlens array within the optical layout. We locate the phase mask after the beamsplitter in one of the two arms of the interferometer. The arm that contains the phase mask is shorter than the other. This is because the phase mask always introduces positive values of OPD and we also need negative values to locate the centre of the interference fringe. We explain the working principle of the phase mask in next section. We are proceeding with several simulations to find, with micrometre accuracy, the location for all the optical components of the metrology instrument. In Fig. 2 we present a first schematic drawing of the interferometer. While at Fig. 3 there is the lenses array before the beamsplitter to ensure that the FOV passes through each step of the phase mask. There is one lens of the microlens array associated with each step of the phase mask.

2.4 Working principle of the phase mask

The metrology instrument incorporates an innovative phase mask to perform dynamic or single-frame white light interferometry. The objective is to have at the detector a set of interferograms of the same mirror area at different OPD. The phase mask is within an optical layout that ensures that the entire FOV passes by all the

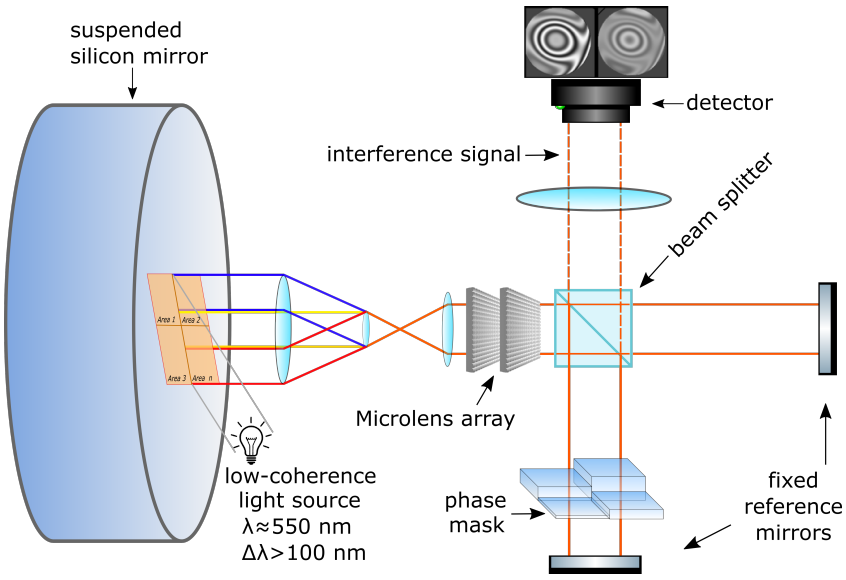

Figure 2. Schematic optical layout of the metrology instrument to measure the topology change and local vibration of the suspended silicon mirror.

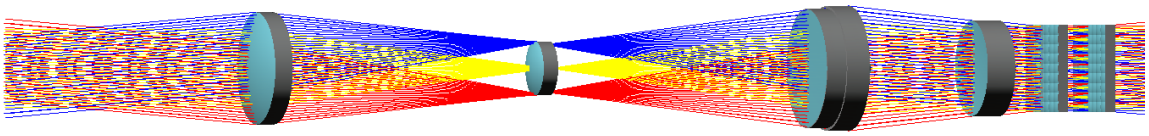

Figure 3. CODE V optical simulation of the focusing lens at the beginning of the metrology instrument. We use the microlenses to sample the signal. One lens of the microlenses is associated with one step of the phase mask. The objective is to obtain an interferogram of the same mirror area for each step of the phase mask.

steps. Then, we can reconstruct the individual white light interferograms for each of the points inside the area observed.

The phase mask we conceive has a step design, where each step simulates the change in Optical Path Difference (OPD) introduced by the displacement of a PZT device. Each step is made of the same material but has a different thickness. If we consider two monochromatic light rays, Eq. 4 gives the OPD between the rays when one traverses a material with a thickness e, and the other displaces parallel on air. n is the material index of refraction for a wavelength.

$$OPD = e \cdot (n - 1) \tag{4}$$

In our case, we use a polychromatic source, and therefore the phase shift is not equal for all the wavelengths. We are looking for the best way to reduce the consequent chromatic aberrations by implementing two complementary masks made each from a different material.

Figure 4 contains a schematic representation of the mask working principle.

The vertical resolution desired determines the number of steps needed for the phase mask and the height difference or phase shift between steps.

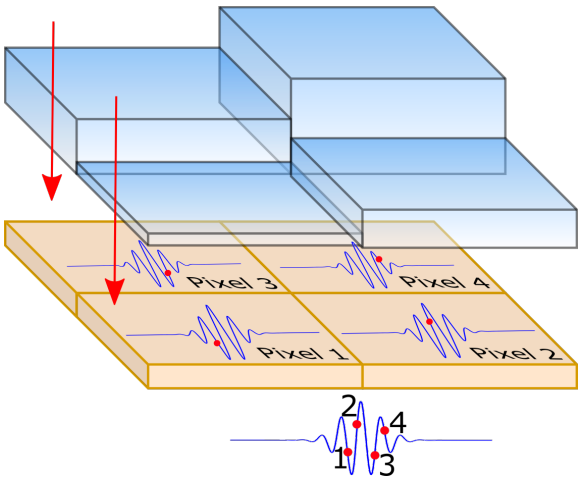

Figure 4. Concept view of the phase mask designed to perform single-frame white light interferometry.

2.5 Determination of the peak of the coherence envelope

The feasibility of the phase mask manufacturing is a critical parameter for us. We look for the lower number of steps and a significant height difference between them. As a result, we discard the centroid method that estimates the position of the zero-order fringe with the centre of gravity, the centroid, of a considerable set of points. Then, again a large number of data points and big computation times are the reasons to not considered for the moment the frequency-domain analysis methods.[3] In the latter technique, the interference data is transformed into the frequency domain by Fourier analysis and then the relative surface height is determined by calculation of the rate of change of the interferometric phase with the wavenumber.[4] Moreover, to simplify the optical layout and avoid intensity losses through the polarizers, we also discard the possibility of doing a phase shift by a change in the polarization state of the light beam. Our next step was to implement the Phase Shifting Interferometry (PSI) method commonly used in long coherence interferometry. The PSI method computes the relative path difference between the interferometer arms with the interference beam phase. We obtain the phase value with the so-called PSI algorithms, like the one presented in Eq. 5.[15] The PSI algorithms use the intensity of the interference beam measured at different positions of a PZT device. In our metrology instrument, it is the intensity value captured at consecutive steps. These intensity values must be measured with an exact phase shift between them. Equation 5 requires a phase shift of $\lambda/8$ or $\pi/4$ between measurements. Several references define different algorithms with more or fewer points, each one with a specific phase shift.[9]

$$\phi = \tan^{-1}\left[\frac{2\left(I_2 - I_4\right)}{2I_3 - I_5 - I_1}\right] \tag{5}$$

Despite the effectiveness of this method, we were not able to obtain acceptable results. This is because we use a phase mask that introduces a phase shift by steps of different thicknesses and a polychromatic source. The phase shift depends on the material index of refraction that depends on the wavelength. As a result, we need flexible and compatible methods with the phase mask we develop. One of the methods we use determines the peak of the coherence envelope by a Hilbert transform. Then, we also define a function based on the product of a cosine and a Gaussian function to fit the intensity points. We illustrate this last method in Fig. 5. On this figure, we normalize the intensity again from -1 to 1, knowing that the intensity value is always positive. Moreover, we continue defining and comparing new mathematical functions and analysis methods for precise peak detection to determine which one works better for different measurement conditions.

3. RESULTS

The interferogram associated with each step of the phase mask contains the information of the deformation and local vibration of multiple points inside the area observed on the mirror. Fig. 6 a) illustrates the concept of the

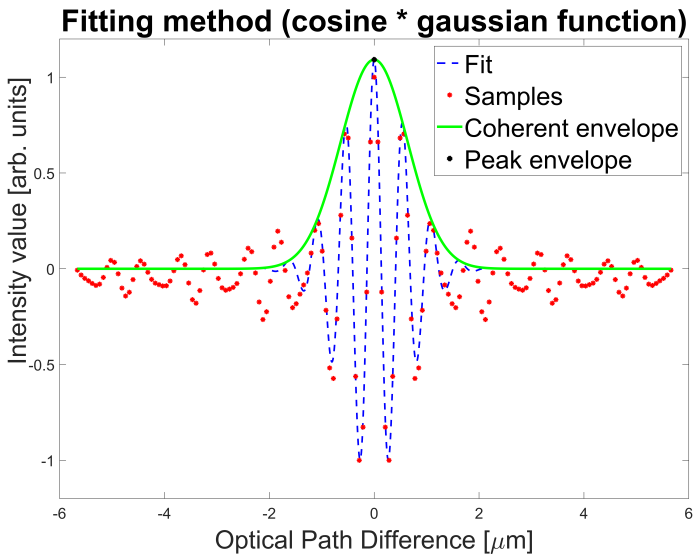

Figure 5. Determination of the peak of the coherence envelope by fitting a mathematical function to the samples. We obtain each sample with a different step of the phase mask.

metrology instrument through a simulation of the interferometer in the optical software ASAP NextGen. This figure represents the four interferograms of the example of mirror deformation of Fig. 6 b) obtained with a phase mask of four steps. We highlight how the entire area observed on the mirror is imaged at each step. For this simulation, we used a spectrum from 400 nm to 600 nm and a central wavelength of 550 nm. Then in Fig. 6 c) we illustrate the reconstruction of the white light interferogram for one of the points inside the area observed. The instrument lateral resolution will be in the order of a few micrometres, according to the pixel size of the detector.

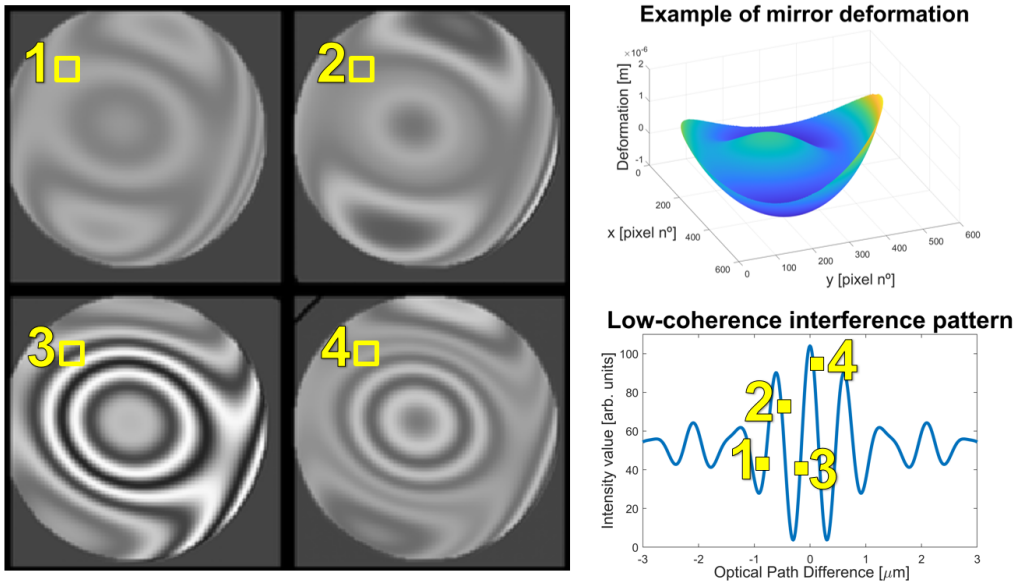

Figure 6. a) ASAP NextGen optical simulation of the interferograms obtained with a phase mask of four steps of the example of mirror deformation (b). c) Reconstruction of the interference pattern for one point. White light source: $\Delta\lambda$ = 400 nm to 600 nm; λ_c = 550 nm.

4. DISCUSSION

The distance between the mirror surface and the first optical element of the metrology instrument is close to 3 m. As a result, we are putting a significant effort into collimating a white light source over 3 m. The size of the vacuum chamber window that connects the mirror with the metrology instrument will be between 1 cm to 3 cm in diameter. The extreme cryogenic temperatures needed inside the vacuum chamber constrain the window size. It is under study the possibility of having several small windows. The pressurization of the vacuum chamber when cooling down the mirror may affect the exterior window and produce aberrations in the measurements.

The method to detect the peak of the coherence envelope determines, first, the number of steps of the phase mask and, second, the height difference between them to reach a specific resolution. We aim for a sub-nanometer resolution on the detection of the local vibration. The coherence region is in the order of a few micrometres. To ensure that the zero-order fringe is within the range of the phase mask, we aim for a notable height difference between the first and the last step of the phase mask. To estimate the location of the coherence region, we propose the alignment of the short-coherence source with a large-coherence source. This is because with a monochromatic source is easier to find the fringes of interference. Additionally, we can use the large-coherence source to complete the topology changes measurements.

The proof of concept under development in the laboratory includes a short-coherence and a set of bandpass filters. These bandpass filters have a progressively wider bandwidth to test the limits on the zero-order fringe detection.

5. CONCLUSION

We presented the state of the development of the metrology instrument and the characterization we want to do on the mirror. We explain some of the methods that we are applying to solve the problem of a topology change and vibration during the cooling down. The next step will be the final definition of the mask and its tolerancing to proceed with its manufacturing. For this project, we still need to do a large research effort to validate some of the concepts presented. The characterization we study is essential for the future Einstein Telescope according to the precision expected on the telescope.

ACKNOWLEDGMENTS

The E-TEST project is carried out within the framework of the Interreg V-A Euregio Meuse-Rhine Programme, with 7,5 million euros from the European Regional Development Fund (ERDF). By investing EU funds in Interreg projects, the European Union is investing directly in economic development, innovation, territorial development, social inclusion and education in the Euregio Meuse-Rhine .

REFERENCES

[1] Einstein Telescope Science Team, "Einstein gravitational wave Telescope Conceptual Design Study," tech. rep. (2011).

[2] Kaneda, H., Nakagawa, T., Enya, K., and Onaka, T., "Cryogenic optical testing of SIC mirrors for ASTRO-F and C/SIC composite mirrors for SPICA," *European Space Agency, (Special Publication) ESA SP* (554), 699–706 (2004).

[3] Sandoz, P., Devillers, R., and Plata, A., "Unambiguous profilometry by fringe-order identification in white-light phase-shifting interferometry," *Journal of Modern Optics* **44**, 519–534 (1997).

[4] De Groot, P. and Deck, L., "Surface profiling by analysis of white-light interferograms in the spatial frequency domain," *Journal of Modern Optics* **42**(2) (1995).

[5] Deng, Y. and Chu, D., "Coherence properties of different light sources and their effect on the image sharpness and speckle of holographic displays," *Scientific Reports* **7**, 1–12 (2017).

[6] Millerd, J. E. and North-Morris, M., "Dynamic interferometry: measurement of space optics and structures," *Optical Measurement Systems for Industrial Inspection X* **10329G** (2017).

[7] Pavliček, P. and Mikeska, E., "White-light interferometer without mechanical scanning," *Optics and Lasers in Engineering* **124** (2020).

[8] Ferrec, Y., Bonnery, G., Brooker, L., Croizé, L., Gousset, S., and Le Coarer, E., "Nanocarb part 1: compact snapshot imaging interferometer for co2 monitoring from space," *International Conference on Space Optics - ICSO 2018* **11180** (2019).

[9] Groot, P. D., "Principles of interference microscopy for the measurement of surface topography," *Advances in Optics and Photonics* **7**, 1–65 (2015).

[10] Woo Jeon, J., Won Jeong, H., Bin Jeong, H., and Joo, K., "High-speed polarized low coherence scanning interferometry based on spatial phase shifting," *Applied Optics* **58**(20), 5360–5365 (2019).

[11] Malacara, D., [*Optical Shop Testing*], Wiley-Interscience, 3 ed. (2006).

[12] Kim, J. H., "High precision signal processing algorithm for white light interferometry," *Sensors* **8**(12), 7609–7635 (2008).

[13] Lehmann, P., "Aspect ratio of elongated polychromatic far-field speckles of continuous and discrete spectral distribution with respect to surface roughness characterization," *Applied Optics* **41**, 10–12 (2002).

[14] Pavliček, P. and Hýbl, O., "White-light interferometry on rough surfaces— measurement uncertainty caused by surface roughness," *Applied Optics* **47**(16), 2941–2949 (2008).

[15] Goodwin, E. P. and Wyant, J. C., [*Field Guide to Interferometric Optical Testing*], SPIE Press, 1 ed. (2006).